Spark-plasma-sintering (SPS) of nanostructured and submicron titanium oxide powders

Angerer, P.; Yu, L. G.; Khor, Khiam Aik; Krumpel, G.

2004

Angerer, P., Yu, L. G., Khor, K. A., & Krumpel, G. (2004). Spark-plasma-sintering (SPS) of nanostructured and submicron titanium oxide powders. Materials Science and Engineering: A, 381(1-2), 16–19.

https://hdl.handle.net/10356/85654

https://doi.org/10.1016/j.msea.2004.02.009

Spark-Plasma-Sintering (SPS) of Nanostructured and Submicron Titanium Oxide powders

P. Angerer[1], L.G.Yu, K. A. Khor[2] , and G. Krumpel[1]

[1] ARC Seibersdorf research, A-2444 Seibersdorf, Austria

[2] School of Mechanical and Production Engineering, Nanyang Technological University,
50 Nanyang Avenue, Singapore 639798
Singapore

Abstract

Spark-Plasma-Sintering (SPS) consolidation of sub-micron and nanostructured titanium oxide (TiO$_2$) powders was performed between 800 and 1000°C for 1 min. The results were compared with conventional sintering techniques performed between 600 and 1000°C for 120 min. The compacted samples were investigated by X-ray diffraction (XRD) and scanning electron microscopy (SEM). This investigation shows clearly that the SPS method is capable to obtain high densities with correspondingly smaller grain-size from the nanostructured TiO2 powder.

Introduction

Achieving fully dense nanostructured bulk samples is of essential significance in various fields of materials engineering due to their particular mechanical, electrical, optical, and magnetic properties. This paper reports the investigation of the sintering process of conventional and nanostructured titanium oxide samples by means of the spark-plasma-sintering method and compares the results with conventional sintering techniques. Titanium oxide has attracted interest due to its applications in photocatalytic [1] and photoelectric devices [2], chemical sensors [3], and optical coatings [4].

Numerous studies have been done on the conventional sintering and densification of nanocrystalline titanium oxide. For example, Hahn et al. [5] observed the microstructural development of conventionally sintered nanocystalline titanium oxide. The investigation of the anatase-rutile transformation was emphasized in the articles of Hague and Mayo [6] and Gribb and Banfield [7].

The spark-plasma-sintering method can be roughly compared with the conventional hot press. Additionally a pulsed electric current is applied directly to the graphite mold. The SPS method comprises three main mechanisms of action: a) the application of uniaxial pressure, b) the application of pulsed voltage, and c) the resistance heating of graphite dies and sample. Nevertheless, an exact interpretation of the microscopic effect of the SPS has not been achieved. A description of this method and its related modifications including a summary of the historical developments is given by Groza & Zavaliangos [8].

Experimental procedure

Two different titanium oxide powders were used: 1) 40 nm Powder (Nanophase Technologies Corp. NanoTek® titanium dioxide powder), containing anatase, only minor amounts of rutile, average particle size 40 nm and a specific surface area of 38 m^2/g according to data from the supplier; 2) 200 nm powder (Kerr-McGee Pigments (Uerdingen, Germany) Tronox® TR110) an anatase powder with an average particle size of 0.20 μm.

The titanium oxides powders were sintered by means of an SPS-1050 apparatus (Sumitomo Coal Mining, Japan).   About 2.5 g to 3.0 g of the as-received powders were loaded without any pressure or sintering aids in a graphite die (15 mm diameter) and punch unit. A low internal pressure (several Pa, air) was applied at the beginning of the sintering experiment. During the sintering process the pressure increases to 300 Pa while reaching maximal temperature. The pressure applied at the punch unit reached a maximum of 7 to 15 MPa. The electric current employed was typically 500A at 700°C and 800 A at 1000°C. The corresponding voltage lies between 3.0 V and 4.5 V, respectively. The electric current was pulsed periodically with 14 pulses /sec (2 of 14 pulses off as a recovery time). The temperature was measured by means of a pyrometer on the surface of the graphite die cylinder. A temperature gradient between the measured temperature and the sample is expected. This measurement problem was discussed by Kamiya [9]. The internal pressure was controlled by a Pirani element. All parameters were monitored during the experiment. The heating rate was at 100°C/min, the dwelling time was 1 min.

For the conventional sintering experiments the powders were precompacted in 15 mm steel dies with 50 MPa. The obtained tablets with relative green densities between 45-57% were sintered afterwards in an electrical furnace (Heraeus, Germany). The heating rate was approx. 20°C /min, and the dwelling time 120 min, respectively.

Characterisation

The determination of the density of the compacted samples was performed using Archimedes´ principle with ethanol as a liquid medium. The values for the relative densities were calculated assuming a theoretical density for rutile of 4.26 g/cm^3. The microstructural investigation of the fracture surface of the compacted samples was conducted by using a scanning electron microscope (SEM) DSM-950 (C.Zeiss, Germany). The acceleration voltage was between 5 and 20kV.

The phase characterisation of the samples and the subsequent crystallite size determination with X-ray powder diffractometry (XRD) were performed using an Philips X´Pert Powder diffractometer (r = 171.9 mm, θ – 2 θ, Bragg-Brentano geometry) using copper K$\alpha_{1,2}$ radiation at 40 kV and 40 mA. This instrument is equipped with an automatic divergence slit, a sample spinner, a diffracted beam curved graphite monochromator, and a scintillation counter. A receiving slit of 0.1 mm (= 0.033° 2θ) and an anti-scatter slit of 4° were selected. On both sides of the sample sollerslits (0.04 rad) were inserted. The measurements were performed in step-scan mode over the range 5 – 85° 2θ with a step size of 0.02° and a counting time of 3 s/step. The crystallite size determination was carried out using Scherrer´s formula in the form

$$d = K \cdot \lambda / ((B\text{-}b) \cdot \cos \theta) \qquad\qquad (1)$$

where d denotes the average crystallite size, K is the shape factor (normally between 0.9 and 1), λ = 1.54056 Å, is the wavelength of the used radiation, B is the peak width (FWHM or integral breadth), b = 0.08 °2θ is the instrumental standard profile width, and θ denotes the diffracting angle. For the determination of d either the main anatase diffraction peaks at 2θ =25.4° (1 0 1), 48.1° (2 0 0) and 62.8° (2 0 4) or the rutile peaks at 2θ =27.5° (1 1 0) , 36.1° (1 0 1) , 54.4° (2 1 1) and 56.7° (2 2 0) were used and an average value for the crystallite size was subsequently calculated.

These XRD-data are not fully consistent with the observed grain size in the SEM. An increasing crystallite size (XRD) corresponds with an even larger growth of the grain size (SEM). This difference can be generated by a possible polycrystalline structure of the rutile grains. For a more precise determination the influence of the distribution of the crystallite

size, the crystallite shape, and internal stress effects should also be considered. The influence of dislocations and stacking faults, which are rarely distributed homogenously and can consequently reduce the coherence length, lower the XRD-obtained crystallite size values. For further discussion of this issue one can refer to the work of Fultz & Howe [10].

Results and Discussion

Figure 1 shows the obtained densities of conventional and nanostructured TiO_2 samples as a function of the sintering temperature. The lower sintering temperature of the TiO_2 nanopowder in comparison to the conventional samples is obvious. At an equal temperature a higher density can be obtained in the nanostructured samples. This difference occurs during conventional sintering as well as in the SPS experiments. Generally the SPS method generates more dense samples than conventional sintering, although the effective temperatures of both methods are difficult to compare due to their different dynamic measurement conditions.

X-ray powder diffraction measurements were performed of each compacted sample. Figure 2 shows the diffractograms for the 40 nm powder before compaction, and after SPS-compaction at 800, 900, and 1000°C, respectively. Here anatase can be observed only in the pristine sample. In the 200 nm powder samples this anatase-rutile transition proceeds between 800°C and 900°C (shown in Figure 3). The conventional sintering experiments perform equivalent results (XRD-traces not shown here). The 200 nm powder shows a higher transformation temperature due to the reduced surface activity in comparison to the 40 nm powder. The transformation rate of the anatase-rutile-transition is proportional to the crystallite coarsening rate of the anatase particles according to [7].

The grain growth behaviour is crucial for this study. In Figure 4 the dependence of the grain growth d / d_0 as a function of the relative density is shown. The values were obtained according to Equation (1), d_0 denotes the crystallite size of the uncompacted powder. The grain growth in the conventional sintering experiments is significantly higher in comparison to SPS-samples with an equivalent degree of densification.

The kinetics of the crystal growth during sintering was also observed. In Figure 5 the logarithm of the grain size d is plotted versus reciprocal absolute temperature (SPS-experiments). The development of the plot corresponding to the spark-plasma-sintered

samples is tolerably linear. This behaviour is correlated to a thermally activated sintering process controlled by diffusion. The surface energy minimisation or decrease represents the driving force of this process.

According to the equation of Arrhenius in the form

$$d = d_0 \cdot A \cdot \exp (E_{act} /RT) \qquad\qquad (2)$$

-where E_{act} refers to the activation energy, R = 8.314 J / k · mol, the universal gas constant, T denotes the absolute temperature, and A the frequency factor. The values for E_{act} of this reaction were deduced 30±10 kJ /mol for the sintering reaction of the 40 nm powder and 63± 13 kJ /mol for the 200 nm anatase powder. Thus the activation energy of the nanopowder is significant lower. At the corresponding conventional pressureless sintering experiments the deviation from the Arrhenius relation is much more evident. Generally, getting more kinetic data would be desirable. However, in the temperature range of 800°C – 1000°C the slope of these curves indicates higher activation energy (~100 kJ/mol) than those in the SPS experiments. At lower temperature the activation energy seems to be lower. A similar behaviour is described by Krumpel [11], where the crystal growth reaction of a hydrothermally synthesized nanostructured rutile was investigated using the same approach. This effect could be generated by a change of the kinetic mechanism of the crystallisation progress.

Conclusions

Sub-micron and nanostructured titanium oxide (TiO_2) powders were consolidated through SPS technique in the temperature range 800 and 1000°C for 1 min.   The results were compared with conventional sintering techniques performed between 600 and 1000°C for 120 min. Results obtained demonstrated the following: (a) Nanostructured TiO_2 samples were densified to a greater extent than the submicron samples at the same temperature in the SPS; (b) Grain growth in the conventional sintering experiments is significantly higher in comparison to SPS-samples at an equivalent level of densification, and (c) The activation energy of the nanopowder was found to be significant lower.

Acknowledgments

References

[1] Iketani, K., Sun, R.-D., Toki, M., Hirota, K., & Yamaguchi, O. (2003). Sol-Gel-derived TiO_2/poly(dimethylsiloxane) hybrid films and their photocatalytic activities. J. Phys. Chem. Solids 64, 507-513.

[2] Barbé, C. J., Arendse, F., Comte, P., Jirousek, M., Lenzmann, F., Shklover, V., & Grätzel, M. (1997). Nanocrystalline Titanium Oxide Electrodes for Photovoltaic Applications. J. Amer. Ceram. Soc. 80 [12], 3157-3171.

[3] Garzella, C., Comini, E., Bontempi, E., Depero, L. E., Frigeri, C., & Sberveglieri, G. (2002). Sol-gel TiO_2 and W/TiO_2 nanostructured thin films for control of drunken driving. Sensors and Actuators B 83 (2002) 230-237.

[4] Kim, D. J., Hahn, S. H., Oh, S. H., & Kim, E. J. (2002). Influence of calcination temperature on structural and optical properties of TiO_2 thin films prepared by sol-gel dip coating. Materials Letters 57, 355-360.

[5] Hahn, H., Logas, J., & Averback, R. S. (1990). Sintering characteristics of nanocrystalline TiO_2. J. Mater. Res. 5 (No. 3) 609 - 614.

[6] Hague, D. C. & Mayo, M. J. (1993). The effect of crystallisation and a phase transformation on the grain growth of nanocrystalline Titania. Nanostructured Materials 3, 61 - 67.

[7] Gribb, A. A. & Banfield, J. F. (1997). Particle size effects on transformation kinetics and phase stability in nanocrystalline TiO_2. Amer. Min. 82, 717 - 728.

[8] Groza, J. R. & Zavaliangos, A. (2000). Sintering activation by external electrical field. Mater. Sci. and Eng. A 287, 171-177.

[9] Kamiya, A. (1998). Observation of sample sintering temperature by the plasma activated sintering (PAS) furnace. J. Mater. Sci. Lett. 17, 49-51.

[10] Fultz, B. & Howe, J. M. (2001). Transmission Electron Microscopy and Diffractometry of Materials, (Springer-Verlag, Heidelberg).

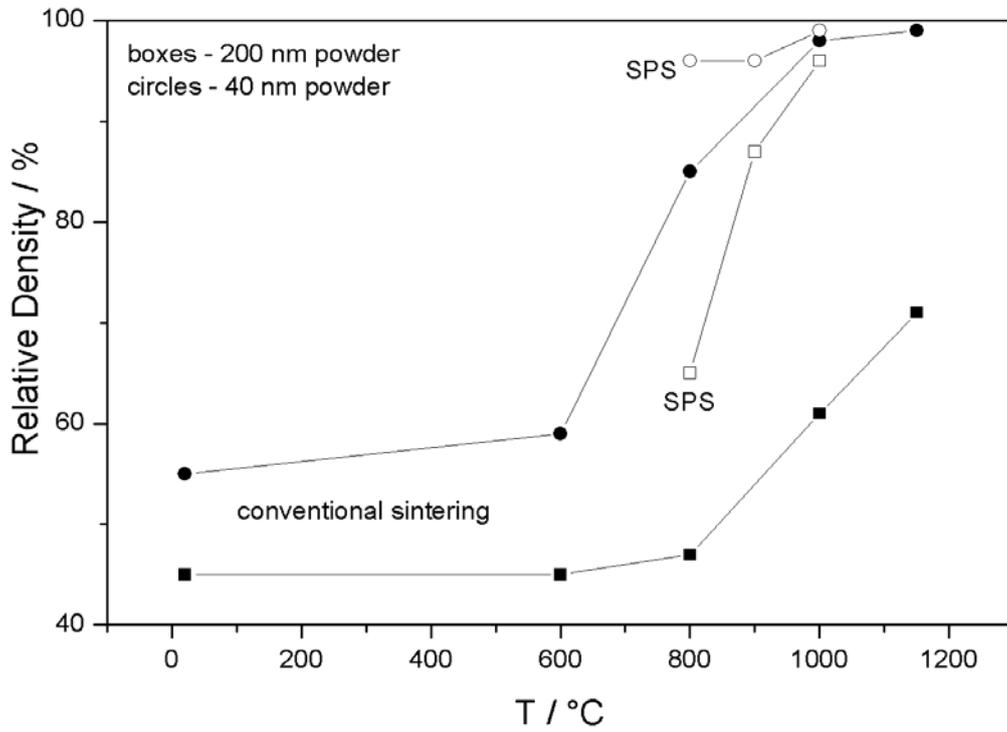[11] Krumpel, G. (2003). Ph.D.Thesis, University of Technology, Vienna.

Figure 1: Relative density as a function of the sintering temperature. The SPS method displays a significant increase of density compared to conventional sintering.
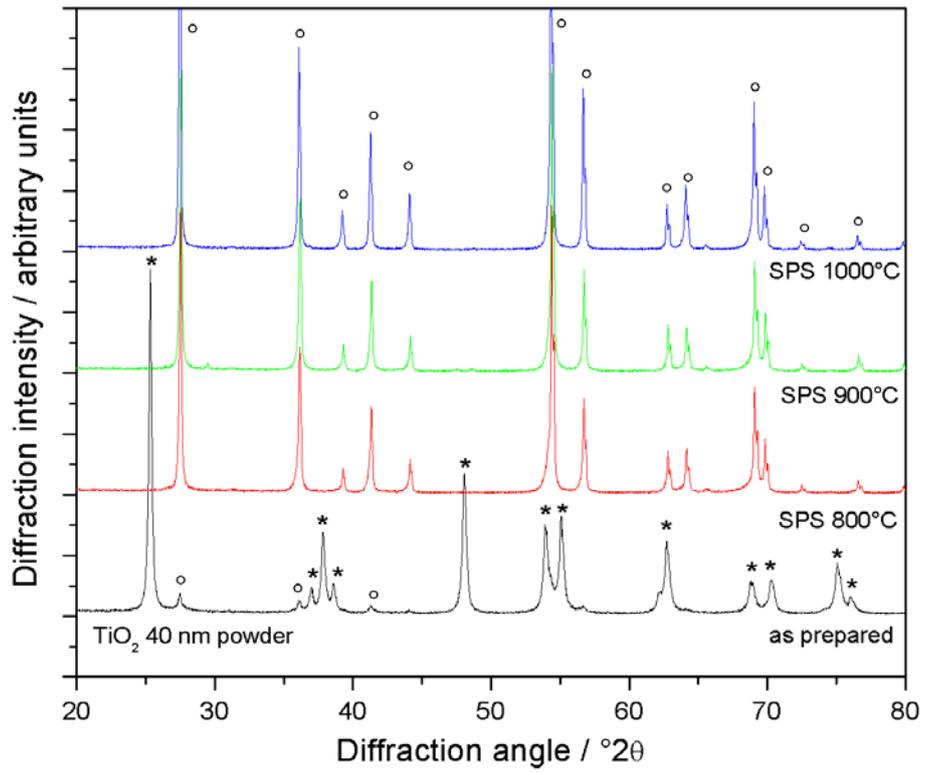
Figure 2: XRD diffractograms of the TiO_2 40 nm powder samples compacted with the SPS method. The transition from anatase to rutile and the decreasing FWHM of the rutile peaks can be identified easily, anatase peaks are denoted by asterisks, rutile peaks by circles.
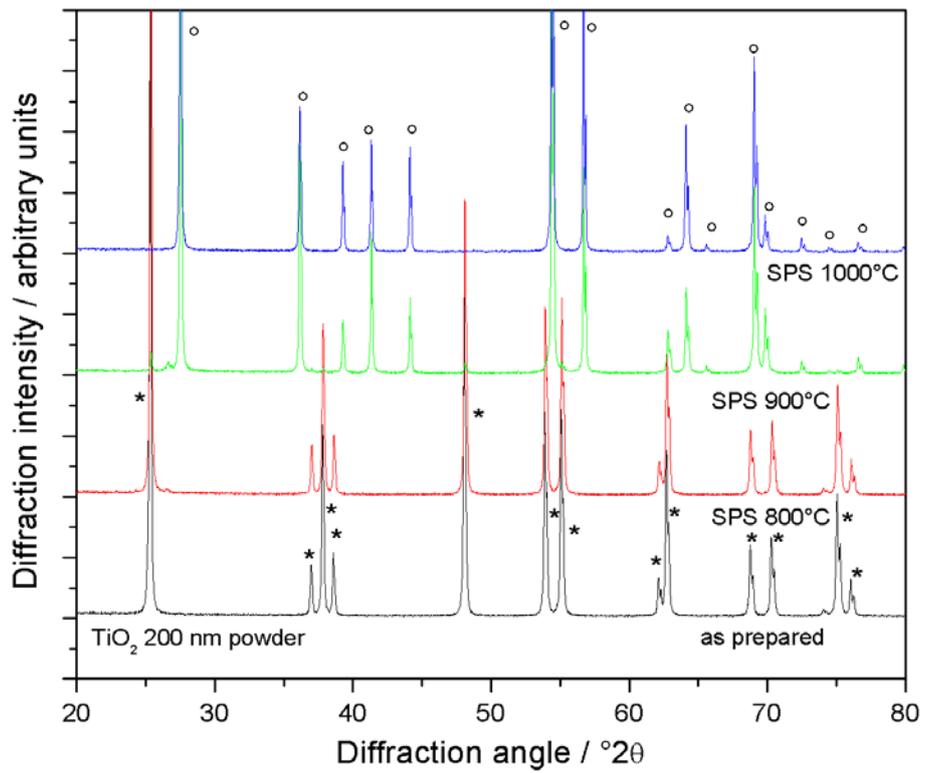
Figure 3: XRD diffractograms of the TiO_2 200 nm powder samples compacted with the SPS method. The transition from anatase to rutile can be identified easily; anatase peaks are denoted by asterisks, rutile peaks by circles.
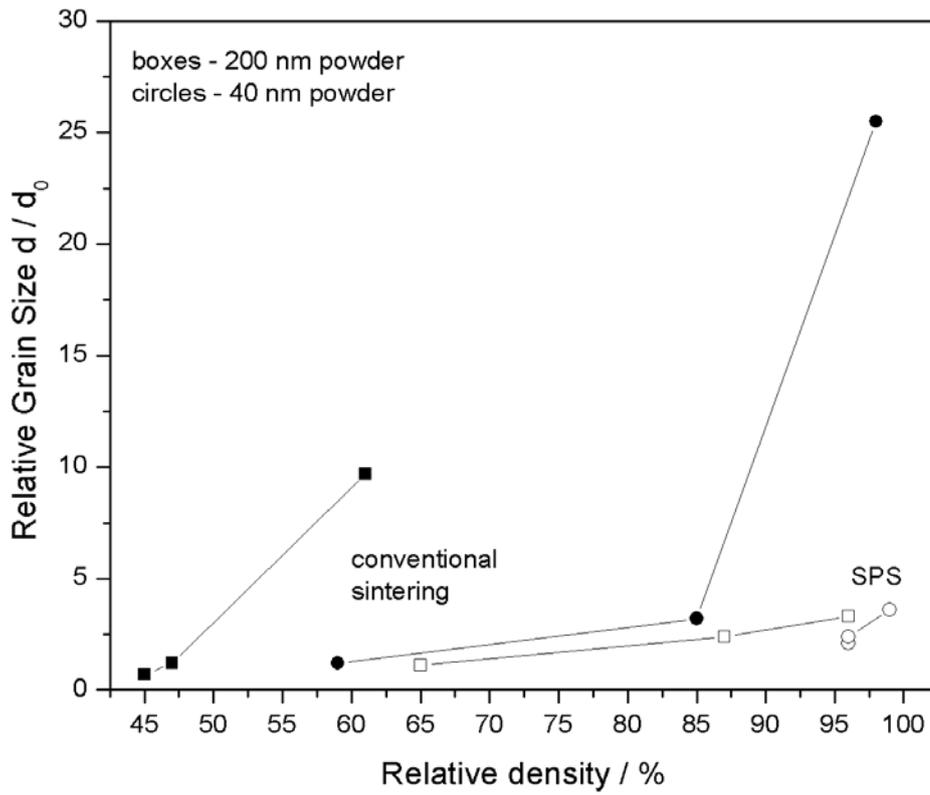
Figure 4: Relative grain size as obtained by XRD, plotted as a function of the relative density. The SPS method shows a significant smaller grain growth.
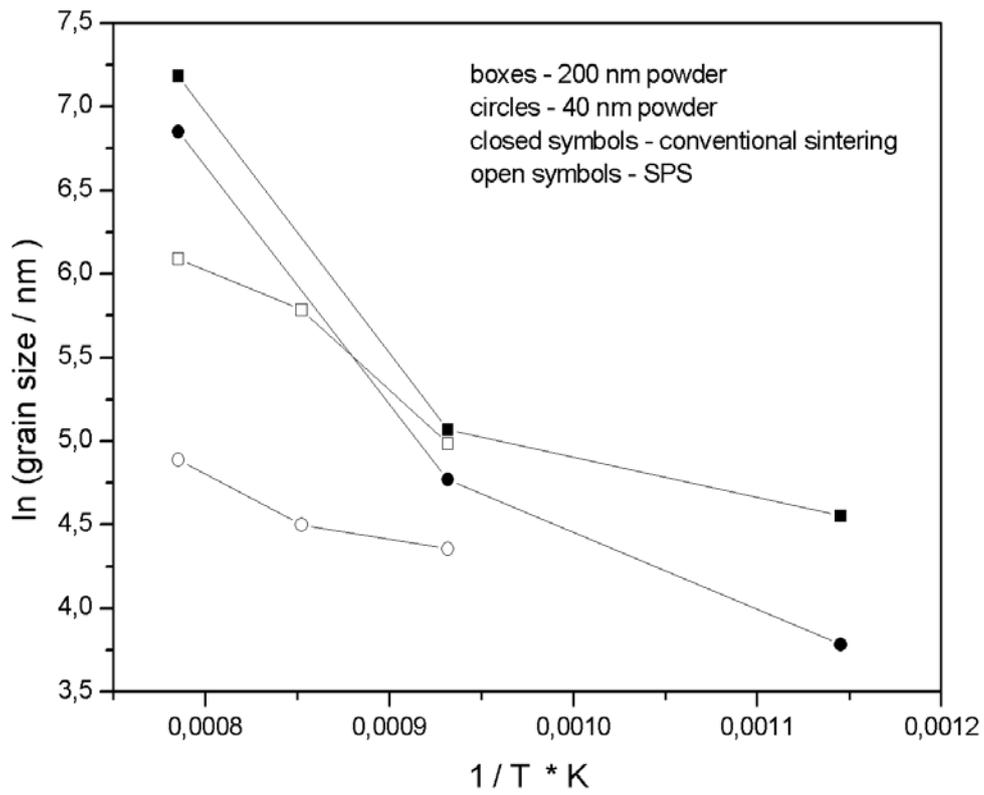
Figure 5: Arrhenius plot of the surface energy activated crystal growth reaction of different TiO$_2$ samples during the SPS compaction and during the conventional sintering process.